Journal of Structural Geology 104 (2017) 1–5

Contents lists available at ScienceDirect

Journal of Structural Geology

journal homepage: www.elsevier.com/locate/jsg

On the use of imaginary faults in palaeostress analysis

Yehua Shan [a, *], Xinquan Liang [b]

[a] Laboratory of Marginal Sea Geology, Guangzhou Institute of Geochemistry, Chinese Academy of Sciences, Guangzhou City 510640, China
[b] State Key Laboratory of Isotope Geochemistry, Guangzhou Institute of Geochemistry, Chinese Academy of Sciences, Guangzhou City 510640, China

ARTICLE INFO

Article history:
Received 20 May 2017
Received in revised form
29 August 2017
Accepted 2 September 2017
Available online 6 September 2017

Keywords:
The right dihedra method
Imaginary fault
Principal stress directions
Dip-slip sense
Tectonic regime

ABSTRACT

The imaginary fault refers to the counterpart of a certain given fault that has a similar expression about the Wallace–Bott hypothesis. It is included to further reduce the feasible fields for the principal stress directions using the right dihedra method. The given fault and its imaginary fault have a similar dip-slip sense under the extensional or compressional regime but, as proved in this paper, a different dip-slip sense under the strike-slip regime. Their relation in dip-slip sense does no change with the rotation of the coordinate system, thus making possible the general use in the reduction of the imaginary faults under any tectonic regime. A procedure for this use is proposed and applied to a real example to demonstrate the feasibility of this method.

1. Introduction

Graphic methods for palaeostress analysis has an advantage of applicability to any set of single-phase newly-formed or reactivated faults, regardless of the fault number and the spread in orientation space of the faults. They include the right dihedra method (McKenzie, 1969; Pegoraro, 1972; Angelier and Mechler, 1977) and the right trihedra method (Lisle, 1987; Ramsay and Lisle, 2000). The former method confines the maximum or minimum principal stress direction to the overlap of the compression or extension field in orientation space bounded by the fault plane and an auxiliary plane perpendicular to the slip line for each individual fault (Fig. 1a). Besides this constraint, the latter method further confines the maximum and minimum principal stress directions to the different dihedra bounded by the auxiliary plane and a second slip–perpendicular auxiliary plane for each fault (Fig. 1b). This criterion requires some a priori knowledge about the principal stress directions, for example, the feasible fields for the principal stress directions using the former method. It is therefore more complicated but more efficient in further reducing the fields.

The relationship between the right dihedra method and the right trihedra method becomes straightforward in the concept of Shan et al.'s (2009) imaginary fault (Fig. 1c). For a certain given fault, the corresponding imaginary fault has a similar slip line and a normal to the null shear stress on the given fault. Both the given fault and its imaginary fault have a similar expression of the Wallace–Bott hypothesis (Wallace, 1951; Bott, 1959). They have a similar normal or reverse dip-slip sense under the extensional (Fig. 2a) or compressional (Fig. 2c) tectonic regime (Shan et al., 2009). In essence, the right trihedra method is equivalent to the application of the right dihedra method to the given and imaginary faults.

However, at present such a use of the imaginary fault requires the a priori knowledge about stress or strain (Shan et al., 2009). For example, for a certain fault with a normal dip-slip sense, the extensional tectonic regime is assumed to determine the dip-slip sense of its imaginary fault. This assumption disregards the possibility that such a fault have formed under the strike-slip regime (Fig. 2b), which limits the use of the imaginary fault.

This paper aims to address the dip-slip sense of the imaginary fault under the strike-slip regime and then to develop a procedure for the general use of the imaginary fault in graphically determining stress under any tectonic regime.

2. Imaginary fault under strike-slip regime

For a certain given fault with a normal, $\boldsymbol{n}$, and a slip line, $\boldsymbol{s}$, the imaginary fault is defined as an auxiliary fault that has the same slip line, and whose plane is perpendicular to the null shear stress direction on the given fault plane, $\boldsymbol{t}$ (Shan et al., 2009). Both faults

* Corresponding author. Tel.: +86 20 85292403; fax: +86 20 85290130.
E-mail address: shanyh@gig.ac.cn (Y. Shan).

https://doi.org/10.1016/j.jsg.2017.09.005
0191-8141/

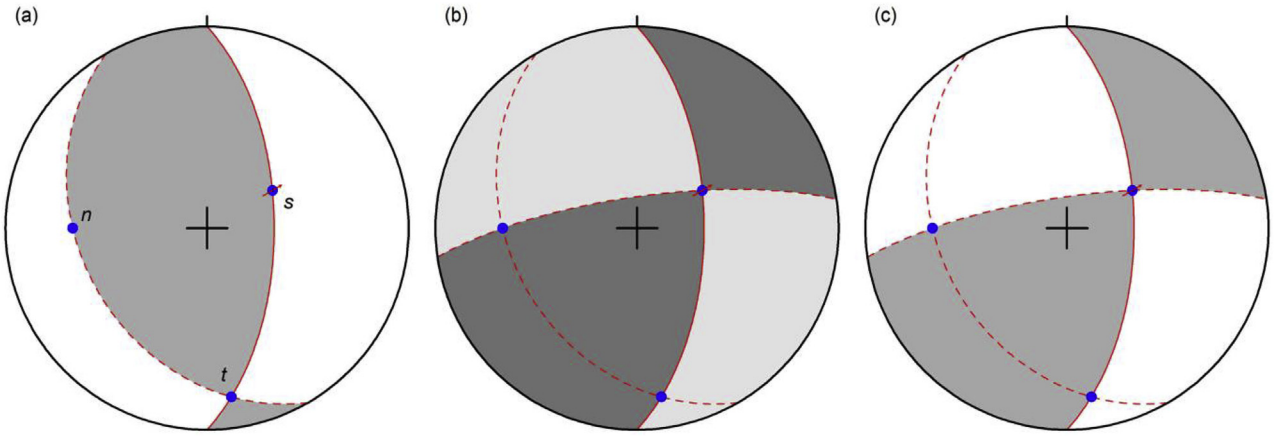

Fig. 1. For a certain given fault with a normal dip-slip sense, the feasible fields of the maximum (grey) and minimum (white) principal stress directions by applying the right dihedra method to it fault (a) and its imaginary fault under the extensional regime (c), respectively, and the two possible right dihedra (dark grey and light grey) for the maximum and minimum principal stress directions in the right trihedra method (b). The given fault has a normal, ***n***, a slip line, ***s***, and a null-shear direction, ***t***. Equal-area, lower hemisphere projection.

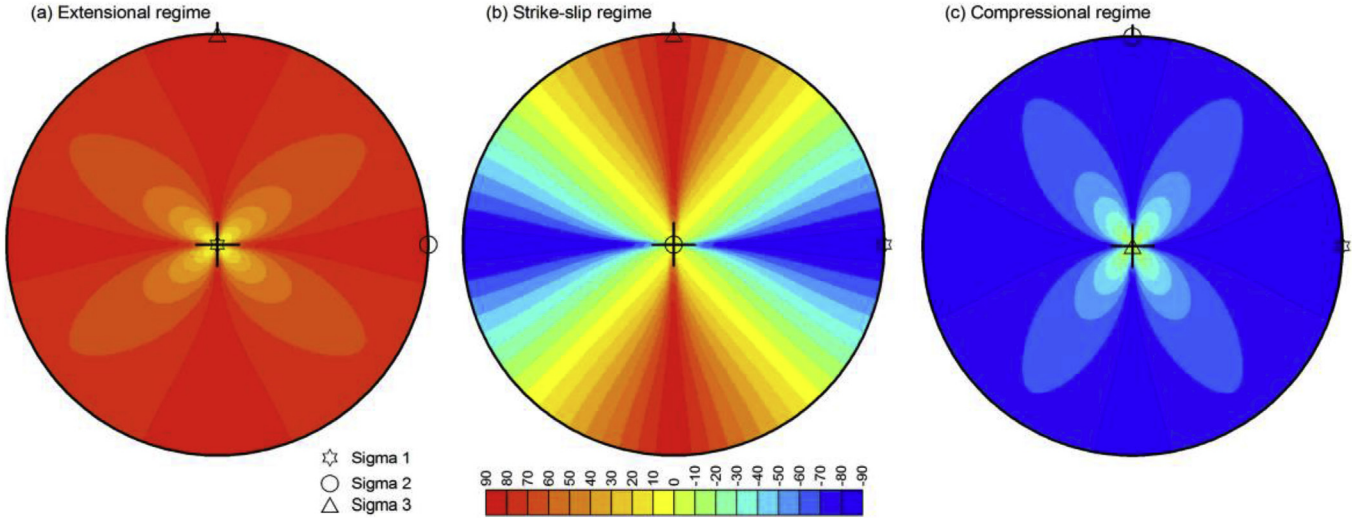

Fig. 2. Distribution of the acute angles between the fault slip lines and the fault strike lines under the extensional (a), strike-slip (b) and compressional (c) regimes, respectively. The angles are displayed at the projection points of the fault dip lines, and have a positive sign for faults with a normal dip-slip sense and a negative sign for faults with a reverse dip-slip sense. The stress ratio is defined as $(\sigma_1-\sigma_2)/(\sigma_1-\sigma_3)$, where σ_1, σ_2 and σ_3 are the maximum, intermediate and minimum principal stress magnitudes, respectively. It is assigned with a constant value 0.5 for these tectonic regimes. Equal-area, lower hemisphere projection.

have a strictly similar expression of the Wallace–Bott hypothesis that there is no traction on the fault plane perpendicular to the slip line, regardless of slip sense:

$$n\cdot\sigma\cdot t = 0, \tag{1}$$

where $\boldsymbol{\sigma}$ is the resulting stress. They have a similar normal or reverse dip-slip component under the extensional (Fig. 2a) or compressional (Fig. 2c) regime (Shan et al., 2009).

For simplicity, the strike-slip regime is represented by the following Andersonian stress,

$$\sigma = \begin{bmatrix} \sigma_1 & 0 & 0 \\ 0 & \sigma_3 & 0 \\ 0 & 0 & \sigma_2 \end{bmatrix}, \tag{2}$$

where σ_i $(i=1,2,3)$ is the principal stress magnitude, and $\sigma_1>\sigma_2>\sigma_3$. In the used Cartesian coordinate system, the first, second and third coordinate axes are directeds eastward, northward and upward, respectively. Compressional or tensile stress is positive or negative in sign throughout this paper.

Let us consider the formation or reactivation of a certain given fault with a normal dip-slip component under the above stress. The fault plane has a unit normal, $n=[\,n_1 \quad n_2 \quad n_3\,]$, where $n_3>0$. In the Wallace–Bott hypothesis, the slip line of the fault is parallel to the shear stress on the fault plane, τ, and is calculated as follows:

$$\tau = \sigma\cdot n - n(n\cdot\sigma\cdot n) = \begin{bmatrix} n_1\left({n_2}^2\Omega_{13}+{n_3}^2\Omega_{12}\right) \\ n_2\left(-{n_1}^2\Omega_{13}-{n_3}^2\Omega_{23}\right) \\ n_3\left(-{n_1}^2\Omega_{12}+{n_2}^2\Omega_{23}\right) \end{bmatrix}^T, \tag{3}$$

where $\Omega_{ij}=\sigma_i-\sigma_j$ $(i,j=1,2,3;\ i\neq j)$, and T is matrix transposition. $\Omega_{ij}\geq 0$ for $i<j$. For the fault with a normal dip-slip component, the shear stress has a positive sign for the third element, τ_3. Consequently,

Table 1
Possible tectonic regimes for the given and imaginary faults with a normal, a reverse or both dip-slip components.

Dip-slip senses		Possible tectonic regimes			
Given faults	Imaginary faults	Extensional	Strike-slip	Compressional	Transitional
normal	normal	✓	–	–	✓
	reverse	–	✓	–	✓
reverse	normal	–	✓	–	✓
	reverse	–	–	✓	✓
normal and reverse	normal and reverse	–	✓	–	✓
	reverse and normal	–	✓	–	✓

$$-{n_1}^2\Omega_{12} + {n_2}^2\Omega_{23} > 0. \tag{4}$$

The fault slip line is represented by $\frac{\tau}{\|\tau\|}$, where $\|\|$ is the vector module.

As is previously defined, the imaginary fault passes through the normal to the considered fault plane and the slip line on it. The normal to the imaginary fault plane, or the null shear stress direction on the fault plane, $\boldsymbol{t}$, is calculated in the following expression:

$$\begin{aligned} t &= n \times \frac{\tau}{\|\tau\|} \\ &= \|\tau\|^{-1}[\, n_2\tau_3 - n_3\tau_2 \quad n_3\tau_1 - n_1\tau_3 \quad n_1\tau_2 - n_2\tau_1 \,]\cdot \\ &= \|\tau\|^{-1}[\, n_2 n_3\Omega_{23} \quad n_1 n_3\Omega_{12} \quad -n_1 n_2\Omega_{13} \,] \end{aligned} \tag{5}$$

In convention, the normal to the imaginary fault plane lies in the upper space. For the sake of convenience, we consider only the case of a positive sign for the third element of $\boldsymbol{t}$, $t_3 > 0$, and then have the below inequality,

$$-n_1 n_2 > 0. \tag{6}$$

Similar to Eq. (3), the shear stress on the imaginary fault plane, τ', also parallel to the slip line of the fault is calculated in the following,

$$\begin{aligned} \tau' &= \sigma\cdot t - t(t\cdot\sigma\cdot t) \\ &= \Omega_{12}\Omega_{23}\Omega_{13}\|\tau\|^{-3}\begin{bmatrix} {n_1}^2 n_2 n_3\left({n_2}^2\Omega_{13} + {n_3}^2\Omega_{12}\right) \\ n_1{n_2}^2 n_3\left(-{n_1}^2\Omega_{13} - {n_3}^2\Omega_{23}\right) \\ n_1 n_2{n_3}^2\left(-{n_1}^2\Omega_{12} + {n_2}^2\Omega_{23}\right) \end{bmatrix}^T. \end{aligned} \tag{7}$$

It is redundant to know from Eqs. (7) and (3) the parallelism in shear stress between the given fault and its imaginary fault, τ and τ'. According to In Eqs. (4) and (6), the third element of τ', τ_3', has a negative sign. This means that the imaginary fault possesses a reverse dip-slip component, as is different from the given fault. On the other hand, for a certain given fault with a reverse dip-slip component, we know in a similar way that its imaginary fault owns a normal dip-slip component. Therefore, the given fault and its imaginary fault have a different dip-slip component under the strike-slip regime.

Additionally, in the case of $t_3 < 0$ in Eq. (5), the imaginary fault has a normal of $-\boldsymbol{t}$ rather than $\boldsymbol{t}$. This modification leads to a different sign for both the left side of In Eq. (6) and the right side of Eq. (7), from which we reach the same conclusion. This will not be presented here to save the space of the paper.

3. Imaginary fault under transitional regime

For a certain given fault with a normal or reverse dip-slip sense, the imaginary fault has a similar dip-slip sense under the extensional or compressional regime (Shan et al., 2009) and, as proved in the previous section, a different dip-slip sense under the strike-slip regime. An issue arises about whether such a relation does or does not hold under the transitional regime. Let us rotate the coordinate system to have two or three oblique principal stress axes, analogous to this regime. In the new system, the imaginary fault may have a similar or different dip-slip sense to the given fault whose dip-slip sense does or does not change with the rotation. Take a given fault with a normal dip-slip component for an example. Its imaginary fault with a reverse dip-slip sense before rotation may have a normal or reverse dip-slip sense after rotation, depending upon whether the given fault does or does not change the dip-slip sense. Anyway, such a rotation does not affect the relation in dip-slip sense between the given fault and the imaginary fault. It is therefore not problematic under the transitional regime to incorporate the imaginary fault into the right dihedral method.

4. Procedure

As it is, the combination of the given and imaginary faults with a similar or different dip-slip sense relates to the resulting tectonic regime. For example, there are three possible tectonic regimes, extensional, strike-slip and transitional for faults with a normal dip-slip sense, three possible regimes, compressional, strike-slip and transitional for faults with a reverse dip-slip sense, and only two possible regimes, strike-slip and transitional for faults with normal and reverse dip-slip sense (Table 1). The given faults are used together with their imaginary faults to constrain the feasible fields for the maximum and minimum principal stress directions and then to determine the tectonic regime from them, in the following procedure.

1) Make two sets of the given and imaginary faults. For each given fault, the imaginary fault has a similar or different dip-slip sense in the first or second set (Table 1).
2) Apply the right dihedra method to the sets, respectively, to define the feasible fields for the maximum and minimum principal stress directions.
3) Appraise whether for each set the feasible fields are well constrained or poorly constrained, depending upon that they do or do not explain all of the given faults and their imaginary faults.
4) Determine the tectonic regime from the well constrained feasible field(s) for the maximum or minimum principal stress direction, if there is or are.

5. Application

In order to demonstrate the feasibility of the procedure proposed in this paper, a set of three measured faults with a normal dip-slip sense (Fig. 3) is taken as an example. These faults were chosen from a large number of polyphase faults collected along the

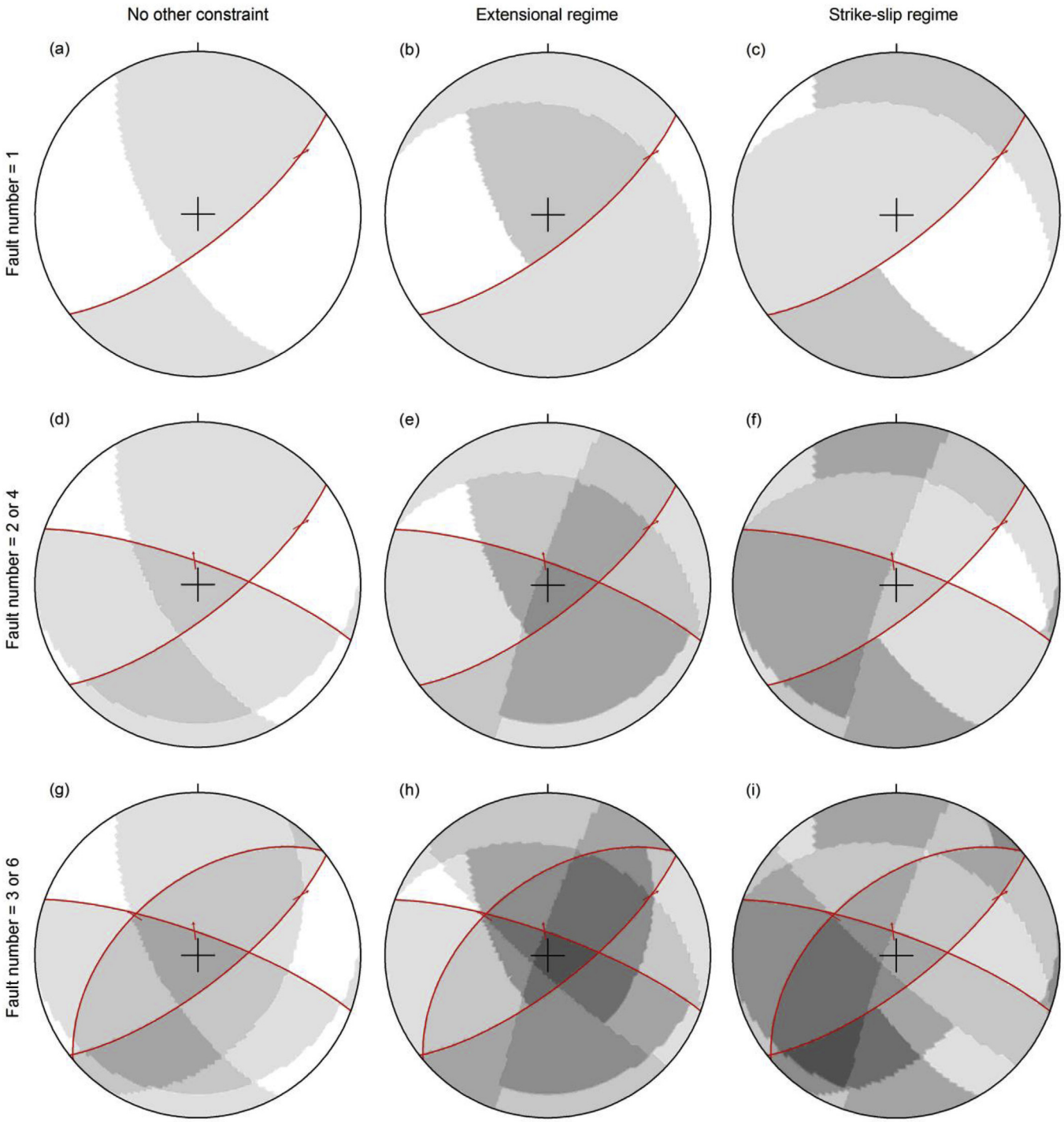

Fig. 3. Graphic determination of the maximum principal stress direction by applying the right dihedra method and the proposed method to a set of one (a–c), two (d–f) and three (g–i) measured faults, respectively. A certain potential field is filled in grey that increases linearly in grey level with the number of faults for the field. In principle, the well-constrained feasible field for the maximum principal stress direction accounts for either the real fault in (a, d and g) or all of the real and imaginary faults in (b, e and h) and (c, f and i); otherwise, it is poorly constrained. In the subfigures, the potential field with a null fault number corresponds with the well-constrained feasible field for the minimum principal stress direction. Equal-area, lower hemisphere projection.

levels of the Xiangdong Tungsten Deposit, Late Jurassic in age (Liang et al., 2016), in central South China. This hypothermal deposit consists of tungsten-bearing quartz veins, nearly vertical and striking toward the northeast or east-northeast. Faults of the chosen kind displaced both the veins and the strike-slip faults occurring on the vein contacts, thus representing a younger, post-mineralization phase of regional extension.

For just one of the faults, the feasible field for the maximum or minimum principal stress direction by applying the right dihedra method to it (Fig. 3a) equals the sum of the feasible fields by applying the right dihedra method to it and its imaginary fault under the extensional (Fig. 3b) and strike-slip (Fig. 3c) regimes, respectively. The latter two fields are similar in size and well constrained; so, we have to accept both of the possible tectonic

regimes.

When another chosen fault is included, the feasible fields for the maximum and minimum principal stress directions by applying the right dihedra method to the two faults (Fig. 3d) and to the two faults and their imaginary faults (Fig. 3e–d) have a smaller size. This becomes more apparent in the latter two cases. In the presence of the well constrained feasible field in the latter two cases, neither of the possible tectonic regimes can be disregarded.

In the case of three chosen faults, both of the possible tectonic regimes are still acceptable, although there is one poorly constrained feasible field for the minimum principal stress direction by applying the right dihedra method to the faults and their imaginary faults under the strike-slip regime (Fig. 3i). Rejecting either of them requires one or more additional fault data. However, the fact that the faults have either a normal dip-slip or a normal oblique-slip (Fig. 3) strongly suggests the preference of the extensional regime. In the well-constrained feasible fields for the maximum and minimum principal stress directions under the extensional regime, the minimum principal stress plunges toward the northwest (Fig. 3h). This is diagnostic of NE-SW regional extension, in relation to the nearly trench-parallel movement of the subducting Pacific oceanic plate to the east during the Cretaceous (Wan, 2011).

6. Discussion

6.1. Advantages and disadvantages

In practice, the proposed method has a smaller amount of computation than the right trihedra method. The former method is a simple application of the right dihedra method to both the faults and their imaginary faults. The latter method also uses the right dihedra method to determine the feasible fields for the principal stress directions for all of the faults, and then reduces these fields by confining the maximum and minimum principal stress direction to the right dihedra bounded by two auxiliary planes for each fault (Lisle, 1987; Ramsay and Lisle, 2000). This reduction is made by comparing the information on the right dihedra for the faults between the meshes of the orientation space. It requires a relatively large memory size and a relatively large calculation time, depending on the mesh number.

The new method is at present inapplicable to two extreme kinds of faults, vertical and strictly dip-slip. Faults of the latter kind have a vertical imaginary fault. It is impossible to use either the normal sense or the reverse sense to describe the dip-slip component of any given or imaginary vertical fault.

6.2. Extreme stress states

In the previous section no consideration is taken into two extreme stress states, $\sigma_1 = \sigma_2 > \sigma_3$ and $\sigma_1 > \sigma_2 = \sigma_3$, in which Eq. (7) predicts no slip line on any imaginary fault, due to the upward direction of σ_2. These states produce a different dip-slip sense for newly-formed or reactivated faults, normal in the former state and reverse in the latter state. They mark the boundaries between the extensional and strike-slip regimes and between the compressional and strike-slip regimes, in the light of the definition of stress in Eq. (2). For a certain given fault, the calculated null-shear direction on the fault plane is $n_2\Omega_{23}\|\tau\|^{-1}[n_3 \quad 0 \quad -n_1]$ in the former state and $n_1\Omega_{12}\|\tau\|^{-1}[0 \quad n_3 \quad -n_2]$ in the latter state, according to Eq. (5). Consequently, for a population of independent faults, their null shear stress directions lie in a great circle that is vertical and east-striking in the former state and vertical and north-striking in the latter state. This great circle has a parallel normal to the minimum and maximum principal stresses, respectively. These features may in turn be used to discriminate the extreme stress states (Ramsay and Lisle, 2000).

7. Conclusions

For any given fault, there is an imaginary fault, with a similar slip line and a normal to the null shear stress direction on the fault, which has a similar expression of the Wallace–Bott hypothesis. Both the given fault and its imaginary fault have a similar dip-slip sense, normal or reverse under the extensional or compressional regime (Shan et al., 2009) and, as this research reveals, a different dip-slip sense under the strike-slip regime. The relation in dip-slip sense between them is not affected by the rotation of the coordinate system. This makes it possible to apply the right dihedral method to the given and imaginary faults under any tectonic regime. A procedure for this general use of the imaginary fault is proposed and applied to a set of three measured faults. Its advantages and disadvantages are discussed.

Acknowledgements

This work is funded by the Strategic Priority Research Program (B) of the Chinese Academy of Sciences (XDB18030104) and the National Natural Science Foundation of China (Grant Nos. 41476035 and 41772206). K. Mulchrone, J.L Simón and two anonymous reviewers provided insightful remarks. This is contribution No. IS-2440 from GIGCAS.

References

Angelier, J., Mechler, P., 1977. Sur une methode graphique de recherche des contraintes principales également utilisable en tectonique et en seismologie: la methode de diédres droits. Bull. Soc. Géol. Fr. 7, 1309–1318.
Bott, M.H.P., 1959. The mechanics of oblique slip faulting. Geol. Mag. 96, 109–117.
Liang, X., Dong, C., Jiang, Y., Wu, S., Zhou, Y., Zhu, H., Fu, J., Wang, C., Shan, Y., 2016. Zircon U-Pb, molybdenite Re-Os and muscovite Ar-Ar isotopic dating of the Xitian W-Sn polymetallic deposit, eastern Hunan Province, South China and its geological significance. Ore Geol. Rev. 78, 85–100.
Lisle, R.J., 1987. Principal stress orientations from faults: an additional constraint. Ann. Tect. 1 (2), 155–158.
McKenzie, D.P., 1969. The relationship between fault plane solutions for earthquakes and the directions of the principal stresses. Bull. Seism. Soc. Am. 59, 591–601.
Pegoraro, O., 1972. Application de la microtectonique à une étude de néotectonique. Le golfe maliaque (Gréce central). These 3éme cycle, Montpellier.
Ramsay, J.G., Lisle, R.J., 2000. The Techniques of Modern Structural Geology Volume 3: Application of Continuum Mechanics in Structural Geology. Academic Press, London.
Shan, Y., Tian, Y., Xiao, W., 2009. Incorporating imaginary faults in graphical stress methods. J. Struct. Geol. 31, 366–368.
Wallace, R.E., 1951. Geometry of shearing stress and relation to faulting. J. Geol. 59, 118–130.
Wan, T.F., 2011. The Tectonics of China: Data, Maps and Evolution. Higher Education Press, Beijing.